A Signal-Multiplexing Ranging Scheme for Integrated Localization and Sensing

Hanying Zhao, *Member, IEEE*, Zijian Zhang, *Student Member, IEEE*, Jian Wang, *Senior Member, IEEE*, Zexu Zhang, and Yuan Shen, *Senior Member, IEEE*

***Abstract*—Precise range information plays a role in acquiring high-precision position awareness, but its accuracy will be severely degraded by clock errors. This letter devises a signal-multiplexing ranging scheme for integrated localization and sensing, which exploits the reflecting non-line-of-sight signals for sensing and jointly determines the node and the target positions with the range estimates. Specifically, we design a ranging protocol with a minimum number of signal transmissions via signal multiplexing and propose a maximum likelihood (ML) range estimate with effective clock error elimination. Simulation results show that the proposed method can achieve centimeter-level accuracy even in the presence of large clock errors.**

***Index Terms*—Integrated localization and sensing, signal-multiplexing ranging, clock drift, cooperation.**

I. Introduction

THE INTERNET-OF-THINGS (IoT) is envisioned to revolutionize the way of what we live and work [1]. In IoT networks, physical objects with sensors, devices, and intelligent computers are integrated and collaboratively collecting, transferring, and processing valuable information. Localization and sensing are core technologies of such cyber-physical systems, which build interfaces between humans and environments and provide position-awareness. However, IoT applications such as logistics and intelligent manufacturing often happen in factories and office environments, where the global positioning system (GPS) fails to provide satisfactory positioning service due to complex propagation channels [2].

Network localization owns the merits of low-cost and flexible coverage and has the potential to achieve cm-level positioning accuracy [3], [4]. In 6G, localization, sensing, and communication will coexist, benefiting from advanced wireless technologies with higher frequencies, wider bandwidth, and massive antenna arrays [5]. High spatial- and temporal- resolutions facilitate multipath separation and inhabited position information extraction, which will change multipath components from foe to friends. The position information is leveraged to construct virtual images of the environments and reshape and control the electromagnetic channels.

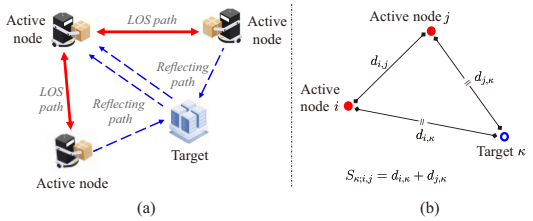

Fig. 1. (a) An illustration of a network with two active nodes and one target; (b) The relationship between absolute range $d_{i,j}$ and sum range $S_{\kappa;i,j}$, where i, j are active nodes and κ is a target.

For integrated localization and sensing systems, synchronization and ranging are tightly coupled, e.g., an *ns*-level clock error will translate to a meter-level ranging error. Traditional synchronization methods such as the alternative double-sided TWR (AltDS-TWR) [6] and the double two-way ranging (TWR) [7] are not efficient, as they require $\mathcal{O}(N^2)$ messages to determine all the node-pair distances for an N-node network. For example, a network with 50 nodes will require over three thousands measuring signals. Since massive signal transmissions lead to long latency, large energy consumption, and heavy hardware complexity, these methods fail to meet the real-time demand for mission-critical applications on the order of tens of milliseconds [8], [9]. In [10], we propose a novel ranging scheme named signal-multiplexing network ranging (SM-NR) for localization systems in line-of-sight (LOS) propagation environments. The notion "signal-multiplexing" is referred to that the signals are transmitted in a broadcast way instead of the conventional point-to-point way in TWR [6], [7]. Our method can fully mitigate clock drifts with a minimum number of signal transmissions for localization, but exploiting reflecting non-line-of-sight (NLOS) signals for sensing requires further investigation.

This letter proposes a signal-multiplexing ranging scheme for integrated localization and sensing, which consists of a ranging protocol with a minimum number of signal transmissions and a maximum likelihood (ML)-based range estimation algorithm with clock error mitigation. In particular, the LOS signals are used for localization and the NLOS signals are employed for sensing. We call this method signal-multiplexing target ranging (SM-TR). Theoretical and numerical results show that the SM-TR can achieve superior

Manuscript received 23 March 2022; accepted 10 April 2022. Date of publication 19 April 2022; date of current version 9 August 2022. This work was supported in part by the Basic Research Strengthening Program of China (173 Program) under Grant 2020-JCJQ-ZD-015-01, and in part by the National Natural Science Foundation of China under Grant 61871256. The associate editor coordinating the review of this article and approving it for publication was H. Yue. *(Corresponding author: Yuan Shen.)*

Hanying Zhao, Zijian Zhang, Jian Wang, and Yuan Shen are with the Department of Electronic Engineering, and Beijing National Research Center for Information Science and Technology, Tsinghua University, Beijing 100084, China (e-mail: hying_zhao@mail.tsinghua.edu.cn; zhangzj20@mails.tsinghua.edu.cn; jian-wang@tsinghua.edu.cn; shenyuan_ee@tsinghua.edu.cn).

Zexu Zhang is with the Deep Space Exploration and Research Center, School of Astronautics, Harbin Institute of Technology, Harbin 150001, China (e-mail: zexuzhang@hit.edu.cn).

Digital Object Identifier 10.1109/LWC.2022.3168433

positioning performance, revealing its potential for integrated localization and sensing systems.

II. Integrated Localization and Sensing Through Signal-Multiplexing

Consider a 2-D network with $N_{\rm a}$ active nodes and denote the index set by $\mathcal{N}_{\rm a} \triangleq \{1, 2, \ldots, N_{\rm a}\}$. These nodes are devices that actively transmit signals for localization and sensing. The position of node n is denoted by $\boldsymbol{p}_n = [x_n \ y_n]^{\rm T} \in \mathbb{R}^2$ for $n \in \mathcal{N}_{\rm a}$, and the position vector of all nodes is written as $\boldsymbol{p} = [\boldsymbol{p}_1^{\rm T} \ \ \boldsymbol{p}_2^{\rm T} \ \cdots \ \boldsymbol{p}_{N_{\rm a}}^{\rm T}]^{\rm T} \in \mathbb{R}^{2N_{\rm a}}$. Meanwhile, there could exist a target κ at position $\boldsymbol{p}_\kappa = [x_\kappa \ \ y_\kappa]^{\rm T} \in \mathbb{R}^2$, which is to be detected by active nodes.[1] In this letter, both $\boldsymbol{p}$ and $\boldsymbol{p}_\kappa$ are of interest.

A. Network Ranging for Localization and Sensing

Due to clock asynchronism, it is necessary to mitigate clock errors for high-accuracy localization and high-quality communication. The SM-TR is designed for integrated localization and sensing, as shown in Fig. 2, where the solid and the dashed arrow lines denote the LOS and the NLOS signals, respectively. Each active node transmits once except for one node, which transmits at the first and the last (i.e., $(N_{\rm a}+1)$-th) time slot. Without loss of generality, assume node 1 transmits twice, and the signal transmission order follows the index number. Eventually, the SM-TR transmits $N_{\rm a}+1$ ranging signals to measure all ranges, and it can be verified that $N_{\rm a}+1$ is actually the minimum number to achieve high-accuracy ranging.[2]

Note that each node will receive not only LOS signals from other nodes but also NLOS single-bounce signals reflecting from target κ. Let $\mathcal{N}_{\rm a}^{(\kappa)}$ denote the set of nodes that can receive signals reflecting from the target. Assume the channel be reciprocal, i.e., the reflecting path from node i to node j is identical to that from node j to i for $i, j \in \mathcal{N}_{\rm a}^{(\kappa)}$, and without loss of generality assume $1 \in \mathcal{N}_{\rm a}^{(\kappa)}$. Note that the latter assumption can be removed when the SM-TR runs periodically, in which case any node in $\mathcal{N}_{\rm a}^{(\kappa)}$ can serve the role of node 1.

Fully-connected networks in which each node pair has a LOS connection are investigated first, and the partially connected networks are then considered in Section II-C. For fully-connected cases, every node will capture timestamps of each signal, either the transmitting time or the receiving time.[3] The range is estimated by measuring the signal propagation time. Let $t_m^{(n,l)}$ $(m \neq n)$ denote the true arrival time of the l-th ($l \in \{1, 2\}$) path of signal m ($m \in \mathcal{N}_{\rm a} \cup \{N_{\rm a}+1\}$) captured by node n. For notation consistency, let $t_n^{(n,1)}$ denote the transmitting time. Using the SM-TR protocol in Fig. 2, the time-of-flight (ToF) between n_1 and n_2 ($n_1, n_2 \in \mathcal{N}_{\rm a}$) takes the form of

$$T_{\rm oF}(n_1, n_2) = \frac{1}{2}\Big(D_{n_1,n_2}^{(n_1,1)} - D_{n_1,n_2}^{(n_2,1)}\Big), \quad \text{for } n_1 < n_2 \quad (1)$$

where $D_{n_1,n_2}^{(n_1,1)} = t_{n_2}^{(n_1,1)} - t_{n_1}^{(n_1,1)}$ characterizes the round-trip time (RTT) and $D_{n_1,n_2}^{(n_2,1)} = t_{n_2}^{(n_2,1)} - t_{n_1}^{(n_2,1)}$ represents the waiting time at node n_2. The range between nodes n_1 and n_2, denoted by d_{n_1,n_2}, is then estimated by multiplying the signal propagation time with the propagation speed c, i.e., $d_{n_1,n_2} = c\, T_{\rm oF}(n_1, n_2)$.

For sensing, let $d_{n,\kappa}$ denote the distance between node n and target κ. From Fig. 1 and Fig. 2, we observe that the time-sum-of-flight (TSoF) of (n_1, κ) and (n_2, κ) for $n_1, n_2 \in \mathcal{N}_{\rm a}^{(\kappa)}$ can be described as

$$T_{\rm s}(\kappa; n_1, n_2) = \frac{1}{2}\Big(D_{n_1,n_2}^{(n_1,2)} - D_{n_1,n_2}^{(n_2,2)}\Big), \quad \text{for } n_1 < n_2 \quad (2)$$

where $D_{n_1,n_2}^{(n_1,2)} = t_{n_2}^{(n_1,2)} - t_{n_1}^{(n_1,1)}$ characterizes the RTT of the NLOS reflecting path and $D_{n_1,n_2}^{(n_2,2)} = t_{n_2}^{(n_2,1)} - t_{n_1}^{(n_2,2)}$ represents the waiting time of NLOS path at node n_2. The range information about the target position is

$$S_{\kappa;n_1,n_2} \coloneqq d_{n_1,\kappa} + d_{n_2,\kappa} = c\, T_{\rm s}(\kappa; n_1, n_2). \quad (3)$$

However, due to non-ideal clocks and observation noises, the timestamp measurements have clock errors, which can be modeled as [12]–[14]

$$\mathsf{t}_m^{(n,l)} = (1 + \mathsf{e}^{(n)}) t_m^{(n,l)} + \theta^{(n)} + \mathsf{w}_m^{(n,l)} \quad (4)$$

where $\theta^{(n)}$, $\mathsf{e}^{(n)}$, and $\mathsf{w}_m^{(n,l)}$ denote the time offset associated with the clock boot time, the clock drift, and the timestamp measurement error, respectively. The clock drift $\mathsf{e}^{(n)}$ is assumed as a random variable bounded by $[-e_{\max}, \ +e_{\max}]$ and is time-invariant within one ranging period [15]–[17].

The goal of this letter is to determine the node and the target positions from the observed timestamp measurements $\mathbf{t} = \mathbf{t}^{\rm L} \cup \mathbf{t}^{\rm NL}$, where

$$\mathbf{t}^{\rm L} = \Big\{\mathsf{t}_m^{(n,1)} \ : \ n \in \mathcal{N}_{\rm a}, m \in \mathcal{N}_{\rm a} \cup \{N_{\rm a}+1\}\Big\} \quad (5a)$$

$$\mathbf{t}^{\rm NL} = \Big\{\mathsf{t}_m^{(n,2)} \ : \ n \in \mathcal{N}_{\rm a}^{(\kappa)}, m \in \mathcal{N}_{\rm a}^{(\kappa)} \cup \{N_{\rm a}+1\}\Big\}. \quad (5b)$$

The clock errors in (4) shall be carefully mitigated.

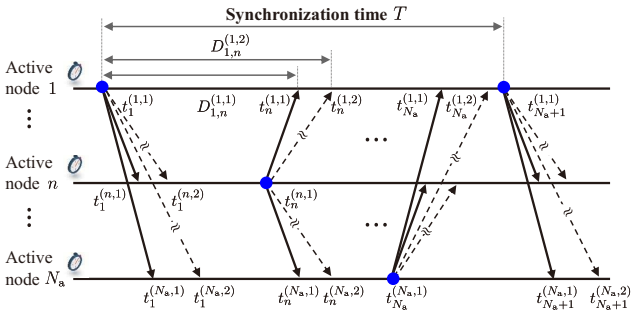

Fig. 2. The protocol of SM-TR for integrated localization and sensing. Each active node transmits once, except node 1 transmits at the first and the last time slot. The horizontal solid lines represent clock timelines. The solid arrow lines characterize the LOS signals, and their dashed counterparts represent the NLOS reflecting signals from the target.

[1]This letter focuses on single-target cases to show the validity of the SM-TR for integrated localization and sensing. For multiple-target scenarios, issues such as multipath identification, data association, and "ghost" target elimination need to be addressed, which is left for future work.

[2]Some nodes can work in the silent mode, which only receives ranging signals from active nodes, to further reduce signal overhead. The distance parameters can be obtained using methods in [10].

[3]Multipath separation methods and timestamp estimation methods are well documented in the literature, such as [11] and references therein, which are not discussed here.

B. Range Estimation

This section develops algorithms for effective clock error mitigation. Recall clock offset $\theta^{(n)}$ in (4), and in parallel to notion $D_{n_1,n_2}^{(n,l)}$ in (1) and (2), define

$$\bar{\mathsf{D}}_{n_1,n_2}^{(n_1,l)} = \mathsf{t}_{n_2}^{(n_1,l)} - \mathsf{t}_{n_1}^{(n_1,1)} \text{ and } \bar{\mathsf{D}}_{n_1,n_2}^{(n_2,l)} = \mathsf{t}_{n_2}^{(n_2,1)} - \mathsf{t}_{n_1}^{(n_2,l)}$$

for $l = 1, 2$, in which $\theta^{(n_1)}$ and $\theta^{(n_2)}$ have been eliminated.

Next, for clock drift $\mathsf{e}^{(n)}$ in (4), we define the transmitting time interval between two LOS signals from node 1 as the *synchronization time*, denoted as T. As shown in Fig. 2, for node $n \in \mathcal{N}_\mathrm{a}\backslash\{1\}$, the receiving time interval between two LOS signals from node 1 and the receiving time interval generated by NLOS signals satisfy

$$\mathsf{t}_{N_\mathrm{a}+1}^{(n,2)} - \mathsf{t}_1^{(n,2)} = \mathsf{t}_{N_\mathrm{a}+1}^{(n,1)} - \mathsf{t}_1^{(n,1)} \coloneqq \mathsf{T}^{(n)}$$

where the first equality implies the feasibility of tackling LOS and NLOS signals in a unified manner. Note that without clock errors, $\mathsf{T}^{(n)} = T$ and we use it for clock drift mitigation. By neglecting the noise term $\mathsf{w}_m^{(n,l)}$, the observations for synchronization time taken from different nodes hold

$$\frac{\mathsf{T}^{(n_1)}}{\mathsf{T}^{(n_2)}} = \frac{\mathsf{k}^{(n_1)}T}{\mathsf{k}^{(n_2)}T} = \frac{\mathsf{k}^{(n_1)}}{\mathsf{k}^{(n_2)}}, \text{ for } n_1, n_2 \in \mathcal{N}_\mathrm{a} \tag{6}$$

where $\mathsf{k}^{(n)} \coloneqq 1 + \mathsf{e}^{(n)}$ with $\mathsf{e}^{(n)}$ in (4). Based on (6), the ToF between node-pair (n_1, n_2) and the TSoF between pairs (n_1, κ) and (n_2, κ) can be rewritten as

$$T_\mathrm{oF}(n_1, n_2) = \frac{T}{2}\left(\frac{\bar{\mathsf{D}}_{n_1,n_2}^{(n_1,1)}}{\mathsf{T}^{(n_1)}} - \frac{\bar{\mathsf{D}}_{n_1,n_2}^{(n_2,1)}}{\mathsf{T}^{(n_2)}}\right),\ n_1, n_2 \in \mathcal{N}_\mathrm{a}$$

$$T_\mathrm{s}(\kappa; n_1, n_2) = \frac{T}{2}\left(\frac{\bar{\mathsf{D}}_{n_1,n_2}^{(n_1,2)}}{\mathsf{T}^{(n_1)}} - \frac{\bar{\mathsf{D}}_{n_1,n_2}^{(n_2,2)}}{\mathsf{T}^{(n_2)}}\right),\ n_1, n_2 \in \mathcal{N}_\mathrm{a}^{(\kappa)}.$$

Hence, the ML ToF estimation $\widehat{\mathsf{T}}_\mathrm{oF}^\star(n_1, n_2)$ and the ML TSoF estimation $\widehat{\mathsf{T}}_\mathrm{s}^\star(\kappa; n_1, n_2)$ can be derived as

$$\widehat{\mathsf{T}}_\mathrm{oF}^\star(n_1, n_2) = \frac{\widehat{\mathsf{T}}^\star}{2}\left(\frac{\bar{\mathsf{D}}_{n_1,n_2}^{(n_1,1)}}{\mathsf{T}^{(n_1)}} - \frac{\bar{\mathsf{D}}_{n_1,n_2}^{(n_2,1)}}{\mathsf{T}^{(n_2)}}\right),\ n_1, n_2 \in \mathcal{N}_\mathrm{a} \tag{7a}$$

$$\widehat{\mathsf{T}}_\mathrm{s}^\star(\kappa; n_1, n_2) = \frac{\widehat{\mathsf{T}}^\star}{2}\left(\frac{\bar{\mathsf{D}}_{n_1,n_2}^{(n_1,2)}}{\mathsf{T}^{(n_1)}} - \frac{\bar{\mathsf{D}}_{n_1,n_2}^{(n_2,2)}}{\mathsf{T}^{(n_2)}}\right),\ n_1, n_2 \in \mathcal{N}_\mathrm{a}^{(\kappa)} \tag{7b}$$

where $\widehat{\mathsf{T}}^\star$ is the ML estimator for synchronization time T, given by

$$\widehat{\mathsf{T}}^\star = \underset{T}{\operatorname{argmax}}\, h_{\mathbf{e}}\Big(\mathbf{t}^\mathrm{L} \cup \mathbf{t}^\mathrm{NL}, T\Big) \tag{8}$$

in which $h_{\mathbf{e}}$ denotes the probability density function (PDF) of random vector $\mathbf{e} = [\mathsf{e}^{(1)}\ \mathsf{e}^{(2)}\ \cdots\ \mathsf{e}^{(N_\mathrm{a})}]$. To better illustrate (8), we let $\mathbf{e}$ be independent and identically distributed with uniform distribution as an example. Then the ML estimator for T in (8) can be derived as

$$\widehat{\mathsf{T}}^\star = \frac{\max\{\mathsf{T}^\mathrm{L}, \mathsf{T}^\mathrm{NL}\}}{1 + e_\mathrm{max}} \tag{9}$$

where $\mathsf{T}^\mathrm{L} = \max_{n\in\mathcal{N}_\mathrm{a}}\{\mathsf{t}_{N_\mathrm{a}+1}^{(n,1)} - \mathsf{t}_1^{(n,1)}\}$ and $\mathsf{T}^\mathrm{NL} = \max_{n\in\mathcal{N}_\mathrm{a}^{(\kappa)}}\{\mathsf{t}_{N_\mathrm{a}+1}^{(n,2)} - \mathsf{t}_1^{(n,2)}\}$.

The range estimate $\widehat{\mathsf{d}}_{n_1,n_2}$ and the sum range estimate $\widehat{\mathsf{S}}_{\kappa;n_1,n_2}$ are obtained by multiplying time estimation in (7) with signal propagation speed c. In particular, by substituting (9) into (7), the errors of estimates $\widehat{\mathsf{d}}_{n_1,n_2}$ and $\widehat{\mathsf{S}}_{\kappa;n_1,n_2}$

$$\omega_{n_1,n_2} = \widehat{\mathsf{d}}_{n_1,n_2} - d_{n_1,n_2}$$
$$\omega_{\kappa;n_1,n_2} = \widehat{\mathsf{S}}_{\kappa;n_1,n_2} - S_{\kappa;n_1,n_2}$$

can be characterized by the following two propositions.

Proposition 1: The worst-case errors of the range estimate $\widehat{\mathsf{d}}_{n_1,n_2}$ and the sum range estimate $\widehat{\mathsf{S}}_{\kappa;n_1,n_2}$ with $\widehat{\mathsf{T}}^\star$ in (7) being (9) are given, respectively, by

$$\max_{\mathbf{e}}\{|\omega_{n_1,n_2}|\} = \frac{2e_\mathrm{max}}{1+e_\mathrm{max}}d_{n_1,n_2}$$
$$\max_{\mathbf{e}}\{|\omega_{\kappa;n_1,n_2}|\} = \frac{2e_\mathrm{max}}{1+e_\mathrm{max}}S_{\kappa;n_1,n_2}.$$

Proposition 2: The root mean square errors (RMSEs) of the range estimate $\widehat{\mathsf{d}}_{n_1,n_2}$ and the sum range estimate $\widehat{\mathsf{S}}_{\kappa;n_1,n_2}$ with $\widehat{\mathsf{T}}^\star$ in (7) being (9) are given, respectively, by

$$\sqrt{\mathbb{E}_{\mathbf{e}}\{\omega_{n_1,n_2}^2\}} = \sqrt{\frac{8}{(N'+1)(N'+2)}}\frac{e_\mathrm{max}d_{n_1,n_2}}{1+e_\mathrm{max}}$$
$$\sqrt{\mathbb{E}_{\mathbf{e}}\{\omega_{\kappa;n_1,n_2}^2\}} = \sqrt{\frac{8}{(N'+1)(N'+2)}}\frac{e_\mathrm{max}S_{\kappa;n_1,n_2}}{1+e_\mathrm{max}}$$

where $N' = \sharp\mathcal{N}_\mathrm{a} + \sharp\mathcal{N}_\mathrm{a}^{(\kappa)}$ with $\sharp(\cdot)$ denoting the cardinality of the set.

Proof: The proofs are omitted due to space constraints. If readers are interested, please refer to [10]. □

Remark 1: It can be verified that the proposed range estimates achieve the same order of magnitude accuracy as the state-of-art ranging methods, but with much lower signal overheads, i.e., $\mathcal{O}(N_\mathrm{a})$ compared to $\mathcal{O}(N_\mathrm{a}^2)$. Moreover, increasing network scale will remarkably ameliorate the estimation accuracy but with a limited overhead increase, which demonstrates the superiority of the proposed SM-TR for large-scale networks. Note also that in comparison with [10] only considering LOS paths, incorporating NLOS components improves the accuracy of $\widehat{\mathsf{T}}^\star$ and hence the range estimates. In a way, such performance gain reveals the significance of integrated localization and sensing.

C. Extension to Networks With Partial Observations

In practice, one node may have LOS connections only with a small number of other nodes. For a node pair that does not have LOS connections, the information about the absolute distance is unavailable, and we refer to these two nodes as disconnected. For such partially-connected networks, the ML estimator for synchronization time T in (8) becomes

$$\widetilde{\mathsf{T}}^\star = \arg\max_{T}\ h_{\mathbf{e}}\Big(\{\mathsf{T}^{(n)}, n \in \widetilde{\mathcal{N}}_\mathrm{a}^{(1)}\}, T\Big) \tag{11}$$

where $\widetilde{\mathcal{N}}_\mathrm{a}^{(1)}$ denotes the set of nodes that have a round-trip with node 1 either in LOS, NLOS or both paths. When the SM-TR only performs once, only nodes in set $\widetilde{\mathcal{N}}_\mathrm{a}^{(1)}$ have been synchronized. To realize whole network synchronization, we

shall run the SM-TR cyclically and then any node can serve the role of node 1 for synchronization.

Particularly, for $\mathsf{e}^{(n)} \sim \mathcal{U}[-e_{\max}, e_{\max}]$, $\widetilde{\mathsf{T}}^{\star}$ in (11) takes the same form as $\widehat{\mathsf{T}}^{\star}$ in (9) except the numerator becomes $\max_{n\in\widetilde{\mathcal{N}}_{\mathrm{a}}^{(1)},l\in\{1,2\}}\{\mathsf{t}_{N_{\mathrm{a}}+1}^{(n,l)}-\mathsf{t}_{1}^{(n,l)}\}$. Then, for node pair (n_1, n_2) ($n_1, n_2 \in \widetilde{\mathcal{N}}_{\mathrm{a}}^{(1)}$) with LOS connection, the ToF estimation is given by

$$\widehat{\mathsf{T}}_{\mathrm{oF}}^{\star}(n_1,n_2)=\frac{\widetilde{\mathsf{T}}^{\star}}{2}\left(\frac{\bar{\mathsf{D}}_{n_1,n_2}^{(n_1,1)}}{\mathsf{T}^{(n_1)}}-\frac{\bar{\mathsf{D}}_{n_1,n_2}^{(n_2,1)}}{\mathsf{T}^{(n_2)}}\right),\quad n_1\in\mathcal{N}_{\mathrm{a}}^{(n_2)}$$

where $\mathcal{N}_{\mathrm{a}}^{(n)}$ denotes the set of nodes that have a LOS connection with node n. For those node pairs that do not have LOS connections, the information on the absolute distance could be acquired after position determination, which will be introduced in Section II-E. As for sensing, the ML TSoF estimator for the target with node pair (n_1, n_2) can be derived as

$$\widehat{\mathsf{T}}_{\mathrm{s}}^{\star}(\kappa;n_1,n_2)=\frac{\widetilde{\mathsf{T}}^{\star}}{2}\left(\frac{\bar{\mathsf{D}}_{n_1,n_2}^{(n_1,2)}}{\mathsf{T}^{(n_1)}}-\frac{\bar{\mathsf{D}}_{n_1,n_2}^{(n_2,2)}}{\mathsf{T}^{(n_2)}}\right)$$

where $n_1, n_2 \in \mathcal{N}_{\mathrm{a}}^{(\kappa)} \cap \widetilde{\mathcal{N}}_{\mathrm{a}}^{(1)}$ and $n_1 \in \mathcal{N}_{\mathrm{a}}^{(n_2)}$.

D. Computational Complexity of SM-TR

The computational complexity of the SM-TR is comparatively low. Specifically, let N'' denote the cardinality of set $\mathcal{N}_{\mathrm{a}}^{(\kappa)}$, which satisfies $N'' < N_{\mathrm{a}}$. We first compute the ML estimator of T, which requires $N''+N_{\mathrm{a}}$ FLOPS as shown in (9). Then, according to (7), computing a ToF or a TSoF estimator requires one multiplication and three division operations. Thus, computing all ToFs and TSoFs requires $4\binom{N_{\mathrm{a}}}{2}+4\binom{N''}{2}$ FLOPS in total. Totally, the computational complexity of the proposed SM-TR is $N''+N_{\mathrm{a}}+4\binom{N_{\mathrm{a}}}{2}+4\binom{N''}{2}$, which is approximately proportional to the square of the number of active nodes, i.e., $\mathcal{O}(N_{\mathrm{a}}^2)$, and is acceptable for commercial devices [16].

E. Integrated Localization and Sensing

Finally, the positions of nodes and target are estimated by minimizing the cost function (10), shown at the bottom of this page, where $\eta_{i,j}$ and $\eta_{\kappa;i,j}$ are the confidences of range estimate $\widehat{\mathsf{d}}_{i,j}$ and sum range estimate $\widehat{\mathsf{S}}_{\kappa;i,j}$, respectively. We solve this location-aware problem in three steps: 1) Applying the multidimensional scaling (MDS) method to determine the initial positions of the active nodes [18]; 2) Adopting grid-search method to determine the initial position of the target; 3) Utilizing Newton's method to minimize the cost function (10).

III. Numerical Results

In this section, we numerically evaluate the effectiveness and the efficiency of the SM-TR for integrated localization and sensing in the presence of clock errors. The popular ranging method AltDS-TWR in [6] is adopted as the benchmark. The clock frequency deviations of all nodes are random variables with uniform distribution $\mathcal{U}[-e_{\max}, +e_{\max}]$. Transmission intervals are set as 1 ms.

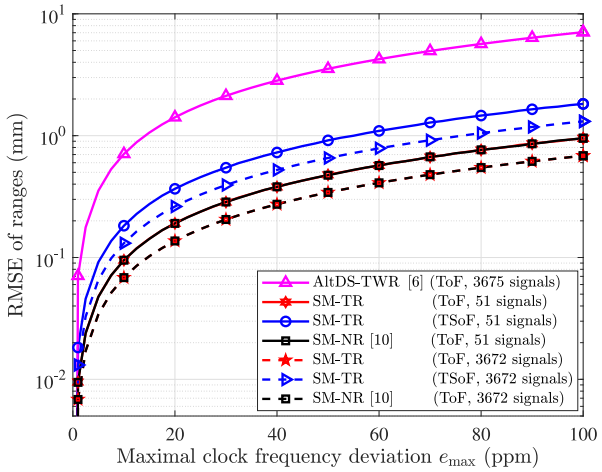

Fig. 3. The RMSEs against the maximal clock frequency deviation.

Consider a network with 50 active nodes and one target randomly distributed in a 300m×300m square. First, note that for this network, the benchmark AltDS-TWR in [6] requires 3675 signals to measure all ranges, while the proposed SM-TR only needs 51 signals. Thus, for a fair comparison, we also perform the SM-TR $\lfloor 3675/51 \rfloor = 72$ times and use the average as the output. The RMSEs of different range estimations against clock frequency deviation are shown in Fig. 3. We observe that in all regions, the sum range estimates for sensing and the range estimates for localization significantly eliminate clock drift effects and attain centimeter-level accuracy, even with much fewer signals. As the clock drift effect becomes severe, all the RMSEs increase, but the SM-TR are notably robust against frequency errors. Moreover, compared with the SM-NR for pure localization [10], the range estimation of SM-TR achieves slightly higher accuracy, demonstrating the benefits of integrated localization and sensing. As for efficiency, the performance of SM-TR with 51 signals is close to that with 3672 signals. Such superior performance verifies the validity of the signal-multiplexing paradigm for sensing.

Next, we investigate the effects of timestamp measurement error on ranging accuracy. We fix the maximal clock frequency deviation $e_{\max}$ as 100 ppm and assume the measurement errors $\mathsf{w}_m^{(n,l)}$ in (4) are Gaussian variables with zero mean and variance σ_w^2. Other system settings remain the same as the previous simulation. The RMSEs of different range estimates as functions of the standard deviation of timestamp measurement error are shown in Fig. 4. We can observe that for both the absolute range and the sum range, the error of estimation is

$$\underset{\boldsymbol{p},\boldsymbol{p}_\kappa}{\text{minimize}}\ \frac{2}{N_{\mathrm{a}}(N_{\mathrm{a}}-1)}\sum_{\substack{i,j\in\mathcal{N}_{\mathrm{a}},\\ i<j}}\eta_{i,j}\left(\|\boldsymbol{p}_i-\boldsymbol{p}_j\|-\widehat{\mathsf{d}}_{i,j}\right)^2+\frac{2}{N''(N''-1)}\sum_{\substack{i,j\in\mathcal{N}_{\mathrm{a}}^{(\kappa)},\\ i<j}}\eta_{\kappa;i,j}\left(\|\boldsymbol{p}_i-\boldsymbol{p}_\kappa\|+\|\boldsymbol{p}_j-\boldsymbol{p}_\kappa\|-\widehat{\mathsf{S}}_{\kappa;i,j}\right)^2 \quad (10)$$

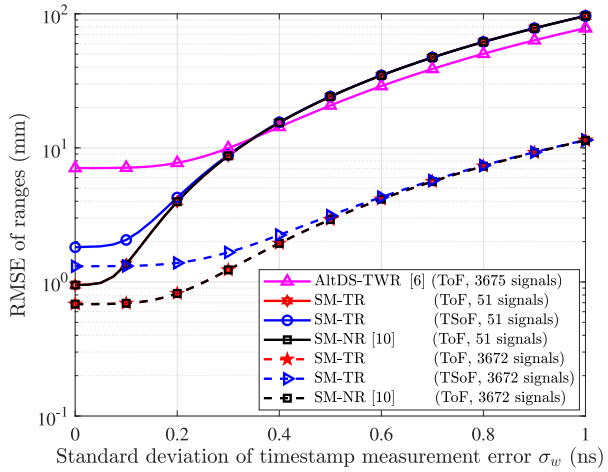

Fig. 4. The RMSEs against the standard deviation of timestamp measurement error.

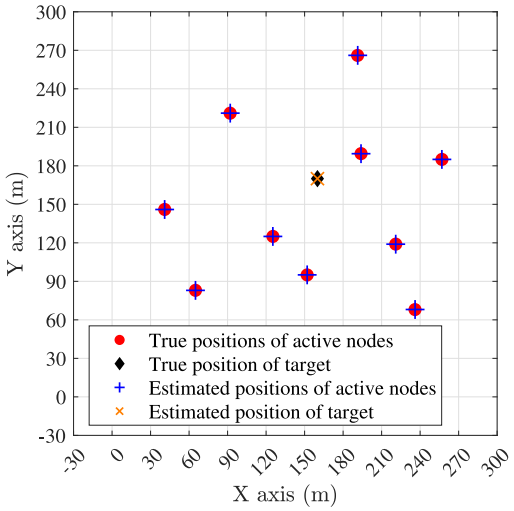

Fig. 5. A network with 10 active nodes and one target.

one order of magnitude lower than other methods. Particularly, when the measurement error is small, the drift errors dominate the clock errors and the SM-TR can effectively mitigate the clock errors. When the measurement errors dominates the clock error, the SM-TR range estimates with 51 measurement signals has inferior performance due to insufficient measurements for mitigation. But as the number of measurements increases, the accuracy dramatically increases and soon outperforms the benchmark. Thus, to alleviate the effect of measurement errors, we can sacrifice certain efficiency to acquire accuracy enhancement. Moreover, we observe that the SM-TR still has higher accuracy than the SM-NR in the presence of measurement errors. These results again demonstrate the advantage of integrated localization and sensing on boosting robustness to clocks errors.

Finally, the positioning performance of integrated localization and sensing algorithm is verified. We consider the random topology in Fig. 5, where the maximal clock frequency deviation is 100 ppm, and the standard deviation of timestamp measurement error is $\sigma_w = 1$ ns. The true and the estimated positions of active nodes and target are shown in Fig. 5. We can observe that both the active nodes and the target are precisely localized with errors less than 10 cm, revealing that the SM-TR provides satisfactory positioning performance even in the presence of clock errors.

IV. Conclusion

This letter proposed a signal-multiplexing ranging scheme for integrated localization and sensing, which exploits reflecting NLOS paths to enable sensing and mitigate clock errors with a minimum number of signal transmissions. Then, an associated ML-based range estimation algorithm as well as an integrated localization and sensing algorithm were further derived. Theoretical analyses and numerical results verified the superiority of the proposed SM-TR in both efficiency and effectiveness. This letter can serve as a guide on adopting the signal-multiplexing paradigm for integrated localization and sensing, which can significantly improve the ranging efficiency especially in large-scale networks.

References

[1] L. Atzori, A. Iera, and G. Morabito, "The Internet of Things: A survey," *Comput. Netw.*, vol. 54, no. 15, pp. 2787–2805, Oct. 2010.
[2] M. Z. Win *et al.*, "Network localization and navigation via cooperation," *IEEE Commun. Mag.*, vol. 49, no. 5, pp. 56–62, May 2011.
[3] M. Z. Win, Y. Shen, and W. Dai, "A theoretical foundation of network localization and navigation," *Proc. IEEE*, vol. 106, no. 7, pp. 1136–1165, Jul. 2018.
[4] H. Zhao, N. Zhang, and Y. Shen, "Beamspace direct localization for large-scale antenna array systems," *IEEE Trans. Signal Process.*, vol. 68, pp. 3529–3544, May 2020.
[5] A. Liu *et al.*, "A survey on fundamental limits of integrated sensing and communication," *IEEE Commun. Surveys Tuts.*, early access, Feb. 7, 2022, doi: 10.1109/COMST.2022.3149272.
[6] D. Neirynck, E. Luk, and M. McLaughlin, "An alternative double-sided two-way ranging method," in *Proc. Workshop Position. Navigat. Commun.*, Banff, AB, Canada, Oct. 2016, pp. 1–4.
[7] H. Kim, "Double-sided two-way ranging algorithm to reduce ranging time," *IEEE Commun. Lett.*, vol. 13, no. 7, pp. 486–488, Jul. 2009.
[8] H. Wymeersch, G. Seco-Granados, G. Destino, D. Dardari, and F. Tufvesson, "5G mmwave positioning for vehicular networks," *IEEE Wireless Commun. Mag.*, vol. 24, no. 6, pp. 80–86, Dec. 2017.
[9] Y. Liu, Y. Wang, J. Wang, and Y. Shen, "Distributed 3D relative localization of UAVs," *IEEE Trans. Veh. Technol.*, vol. 69, no. 10, pp. 11756–11770, Oct. 2020.
[10] Z. Zhang, H. Zhao, J. Wang, and Y. Shen, "Signal-multiplexing ranging for network localization," *IEEE Trans. Wireless Commun.*, vol. 21, no. 3, pp. 1694–1709, Mar. 2022.
[11] H. Zhao, Y. Gong, and Y. Shen, "A multipath separation method for network localization via tensor decomposition," in *Proc. IEEE Int. Conf. Commun.*, Montreal, QC, Canada, Jun. 2021, pp. 1–6.
[12] Y. Wu, Q. Chaudhari, and E. Serpedin, "Clock synchronization of wireless sensor networks," *IEEE Signal Process. Mag.*, vol. 28, no. 1, pp. 124–138, Jan. 2011.
[13] *IEEE Standard for Local and Metropolitan Area Networks—Part 15.4: Low-Rate Wireless Personal Area Networks (LR-WPANs)*, IEEE Standard 802.15.4–2011 (Revision of IEEE Std 802.15.4–2006), pp. 1–314, Sep. 2011.
[14] M. Ouellette, K. Ji, S. Liu, and H. Li, "Using IEEE 1588 and boundary clocks for clock synchronization in telecom networks," *IEEE Commun. Mag.*, vol. 49, no. 2, pp. 164–171, Feb. 2011.
[15] R. Dalce, A. van den Bossche, and T. Val, "A study of the ranging error for parallel double sided-two way ranging protocol," in *Proc. IEEE Semiannu. Veh. Technol. Conf.*, Montreal, QC, Canada, Sep. 2016, pp. 1–5.
[16] C. L. Sang, M. Adams, T. Hörmann, M. Hesse, M. Porrmann, and U. Rückert, "Numerical and experimental evaluation of error estimation for two-way ranging methods," *Sensors*, vol. 19, no. 3, p. 616, Feb. 2019.
[17] K. A. Horváth, G. Ill, and Á. Milánkovich, "Passive extended double-sided two-way ranging with alternative calculation," in *Proc. IEEE Int. Conf. Ubiquitous Wireless Broadband*, Salamanca, Italy, Sep. 2017, pp. 1–5.
[18] I. Borg and P. Groenen, *Modern Multidimensional Scaling: Theory and Applications*. Berlin, Germany: Springer, 2005.